

Development of a MAV -- From Theory to Implementation

Camille PARRA, Bingwei SU, Joel BORDENEUVE GUIBE, Yves BRIERE

Are with the Ecole Nationale d'Ingénieurs de Constructions Aéronautiques, 1 place Émile Blouin, 31056 Toulouse cedex 5
e-mails : cparra@ensica.fr, bsu@ensica.fr, joel.bordeneuve@ensica.fr, yves.briere@ensica.fr

Abstract— A nonlinear model of Pégase, a mini aerial vehicle, is established from the data of wind tunnel test. The interpolation of the force and moment coefficients is introduced. After that, a level straight flight linearization equation is obtained. According to this equation, based on the idea of dynamic inversion, an attitude control law is devised and verified by nonlinear simulation. Later on, the 2-D guidance loop is designed. It includes the altitude control loop and heading control loop. Then a simple attitude determination algorithm is presented. Finally we introduce our experimental setup.

Index Terms— Attitude control, Guidance, MAV, Modelling, Embedded system

I. INTRODUCTION

In order to realise a Mini aerial vehicle (MAV) totally autonomous, we have modelled the Pégase-50 which was developed by ENSICA^[1]. It has a delta-wing configuration with elevator and aileron. Aileron can also be used as elevator. The general characteristics of Pégase are as follows:

- Wing span $b = 0.5m$
- Length $L = 0.34m$
- Wing area $S_{ref} = 0.0925m^2$
- Aerodynamic mean chord $c = 0.185m$
- Speed of cruising $V_0 = 50/60km/h$

Furthermore we have developed an embedded system for this plane which has the capability to acquire flight parameters and to control the MAV, as we'll see at the end of this paper.

II. WIND TUNNEL TEST

So as to obtain the mathematic model of the MAV for designing and evaluating the guidance and control law, wind tunnel test has been carried out in Centre D'essais Aéronautique de Toulouse Soufflerie S4^[2]. At a fixed airspeed, i.e. 20m/s, relationship between three force coefficients, three moment coefficients and angle of attack (α , from -30° to 30°), side-slip angle (β , from 0° to 45°), control surfaces (elevator δ_e : $-5^\circ, 0^\circ, 5^\circ$; aileron δ_a : $0^\circ, 5^\circ, 15^\circ$; or aileron acts as elevator with the deflection of

$-10^\circ, -5^\circ, 0^\circ, 5^\circ$) is presented by the test. That means there exists a map or multi-dimensional function from those four variables to the six coefficients. With these data and inertial moment of the MAV, by proper interpolation, the full degree nonlinear model of Pégase can be obtained.

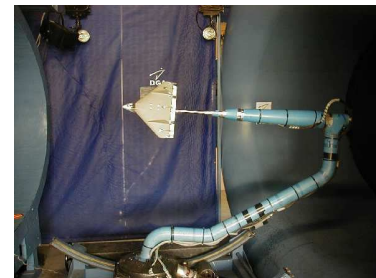


Figure 1 Pégase-50 in the wind tunnel

III. MODELLING

To fulfil the mathematic model, the force coefficients and moment coefficients are needed. They are multi-dimensional function of angle of attack, side-slip angle and control surfaces and can be obtained by interpolation of the discrete values from the wind tunnel test. Four interpolation methods, including linear interpolation, cubic interpolation, nearest neighbour interpolation and spline interpolation had been tested. Linear interpolation had been chosen at last because of the computation speed and interpolation performance consideration.

A. Interpolation of Six Coefficients

Lift coefficient (c_z)

According to the result of wind tunnel test, the angle of attack, side-slip angle and elevator determine lift coefficient while the effect of aileron can be ignored (it can be seen from figure 2). Figure 2 shows the variation of lift coefficient when the position of aileron is $0^\circ, 5^\circ, 15^\circ$ (the position of elevator is set as 0° , side-slip angle is 0°). We can notice that when the position of aileron changes in its whole range, the lift coefficient almost keeps the same value. Therefore by

three-dimensional linear interpolation the lift coefficient can be determined.

Figure 3 is volumetric slice plot of the three-dimensional interpolation result of lift coefficient. The three axes denote the variables of the function and the changing of the colour in the slice denotes the different function value.

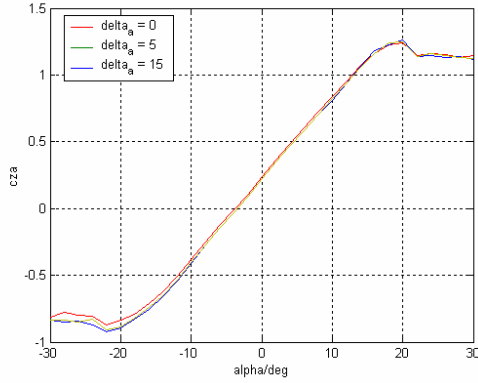


Figure 2 Relation between lift coefficient and aileron

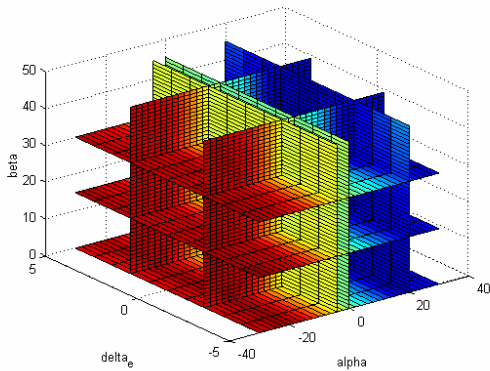


Figure 3 Volumetric slice plot of lift coefficient

By the same idea, the other five coefficients can be obtained. The whole results can be summarized as the following diagram:

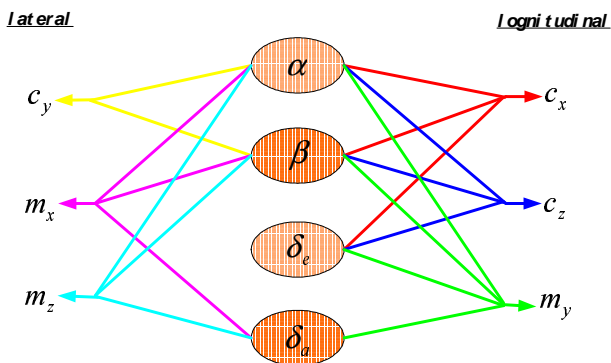


Figure 4 Relationship between aerodynamics coefficient and variables of the wind tunnel test

It can be seen from this diagram that lateral force coefficient (c_y) is determined by angle of attack and side-slip angle, lateral moment coefficients (m_x, m_z) are functions of angle of attack, side-slip angle and aileron while aileron is of little effect on longitudinal forces coefficient (c_x, c_z). However, all the control surfaces make noticeable contributions to pitch moment coefficient (m_y). Thus four-dimensional interpolation needed to obtain this coefficient.

B. Equation of the MAV

From the six coefficients obtained above and the evaluation of inertial moment, a standard twelve-degree nonlinear equation can be derived. The twelve states of the equation are three-dimensional position in earth frame, three velocities in body frame, three body angular rates and the attitude of MAV. Please find the equation in appendix.

IV. CONTROL LAW DESIGN

C. Linearization of the nonlinear equation

It not necessary to use the nonlinear equation to design guidance and control law, therefore considering a level straight flight condition:

$$V_x = 20m/s, V_y = V_z = 0, \theta = \psi = \phi = 0, \delta_e = -4^\circ, \delta_a = 0$$

where V_x, V_y, V_z are velocities of MAV and θ, ψ, ϕ are pitch angle, heading angle and rolling angle. Then the linear equation of this flight state can be obtained:

$$\begin{cases} \dot{q} = -0.02V_x - 2.44V_z - 1.81\delta_e \\ \dot{\theta} = q \\ \dot{p} = -1.47\delta_a \\ \dot{\phi} = p \end{cases}$$

where p is rolling angular rate, q is pitch angular rate. The yaw angle can only be adjusted by the control of rolling angle because only two control variables are available. Suppose that airspeed can be controlled in another close loop, the equation above becomes:

$$\begin{cases} \dot{q} = -1.81\delta_e \\ \dot{\theta} = q \\ \dot{p} = -1.47\delta_a \\ \dot{\phi} = p \end{cases}$$

D. Control law design

Therefore a very simple attitude control law can be obtained by applying the idea of dynamic inversion:

$$\begin{cases} \delta_e = -0.55k_{11}[k_{12}(\theta_d - \theta) - q] \\ \delta_a = -0.68k_{21}[k_{22}(\varphi_d - \varphi) - p] \end{cases}$$

where $k_{11}, k_{12}, k_{21}, k_{22}$ are control parameters to guarantee enough bandwidth and θ_d, φ_d are desired attitude of the MAV. In fact, the close loop poles are

$$\frac{-k_{i1} \pm \sqrt{k_{i1}^2 - 4k_{i1}k_{i2}}}{2}, i = 1, 2$$

E. Airspeed controller design

To guarantee the performance of attitude control, airspeed must be controlled accurately. A PID propulsion controller is designed as:

$$\begin{aligned} Th_c &= mg \sin \theta + D + \mathbf{K}_{dv}^T \dot{\mathbf{V}}^D + \mathbf{K}_v^T (\mathbf{V}^D - \mathbf{V}_A) \\ &+ \mathbf{K}_{\Delta P}^T (\mathbf{P}^D - \mathbf{P}_A) \end{aligned}$$

Th_c is the propulsion command; m denotes the mass of the MAV; g is gravity acceleration; $\mathbf{K}_{dv}, \mathbf{K}_v, \mathbf{K}_{\Delta P}$ are three weight vectors; $\dot{\mathbf{V}}^D, \mathbf{V}^D, \mathbf{P}^D$ are required acceleration, velocity and position vectors; $\mathbf{V}_A, \mathbf{P}_A$ are actual velocity and position Vectors; D is drag force.

F. Simulation results

Nonlinear simulation has been done to verify the effectiveness of attitude controller. The following figure 5 shows the step input response of pitch angle and rolling angle. At the same time, the variation of angle of attack, side-slip angle, control surfaces, heading angle and height are also given.

From the nonlinear simulation, conclusions can be drawn:

- The close loop attitude system is stable, the control law is effective.
- Heading can be controlled by adjusting rolling angle.
- There is an error in pitching channel.

V. 2-D GUIDANCE

The aim of the guidance system is to control the heading of the MAV and to control the lateral position between actual trajectory and desired trajectory when the MAV keeps a certain height. Thus, the guidance system includes *altitude holding loop*, *lateral position control* and *heading control* which are based on the inner loop of attitude control. It is a kind of *two-dimensional* guidance. The guidance algorithm is simple, effective and easy to be implemented.

G. Altitude holding control

The error of desired and actual height is introduced to the pitch angle control loop to constitute the altitude holding control loop. A saturation function is needed to limit the maximum value of feedback terms. Therefore the deflection command of elevator won't exceed its position limit. The altitude holding control law is:

$$\begin{aligned} \delta_e &= -0.55k_{11}[k_{12}(\theta_d - \theta) - q] \\ &+ k_h \text{sat}(H - H_0) \end{aligned}$$

where H denotes the actual height of the MAV; H_0 is the desired height; $\text{sat}(\bullet)$ denotes saturation function.

H. Heading control

Heading angle and the lateral distance between airplane and desired flight trajectory can be controlled by adjusting rolling angle. Based on this idea, lateral guidance law can be obtained. Saturation function is used here for the same reason as in altitude holding control loop. The heading control law is:

$$\begin{aligned} \delta_a &= -0.68k_{21}[k_{22}(\varphi_d - \varphi) - p] \\ &+ k_\psi \text{sat}(\psi - \psi_d) + k_{\Delta y} \text{sat}(\Delta y) \end{aligned}$$

where Δy denotes the lateral distance error.

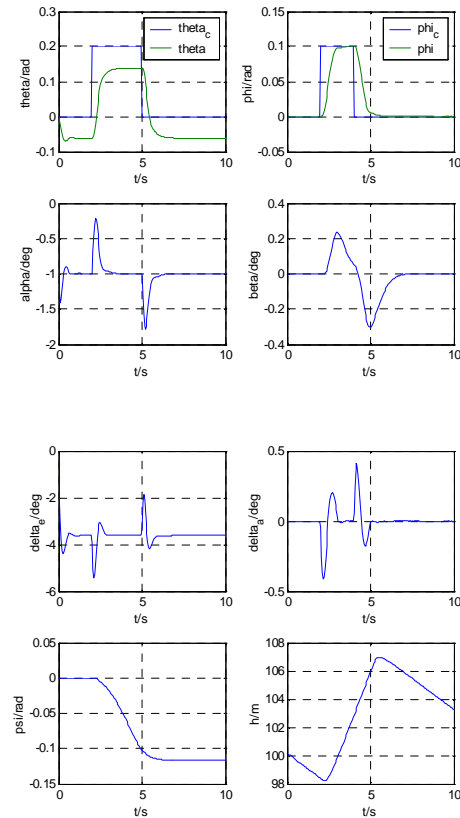


Figure 5 Simulation results for attitude control

VI. ATTITUDE DETERMINATION

To accomplish autonomous guidance and control, the following signals are needed: *three attitude angles*, *angular rates* and *real-time position*. In the design stage of guidance and control law of the MAV, it is supposed that the full states feedback is available. However, in actual flight the position and attitude information can only be obtained by certain navigation sensors on board, including GPS, accelerometer, gyrometers and magnetic

sensor, etc. The limited volume of the MAV and the capability of the CPU on board prevent us from using the mature algorithm whose computation burden is too much to be affordable to determine the attitude. Therefore a simple enough algorithm with certain accuracy must be devised by using those sensors. The following diagram is a basic scheme to determine attitude. According to this scheme, first of all, we must try to compute the rolling angle by the output of accelerometer with the aid of GPS; next, using the output of gyroscope and the value of rolling angle, through certain flight mechanic, pitch angle can be determined; last, heading angle can be derived by compensating the output of magnetic sensor with pitch and rolling angle. Thus, the attitude of MAV is available. This algorithm has been verified in simulation with the 2-5 Hz data rate GPS.

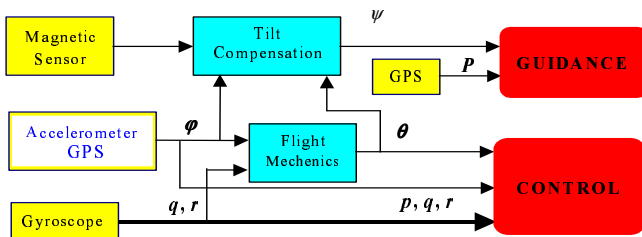


Figure 6 Attitude determination scheme

VII EXPERIMENTAL SETUP

In order to validate the model, the attitude determination algorithms and the control laws, we have conceived and manufactured a compact embedded system that is able to acquire several flight parameters, such as acceleration, angular speed, magnetic field coordinates, position, speed and altitude. The system is shown by figure 7.

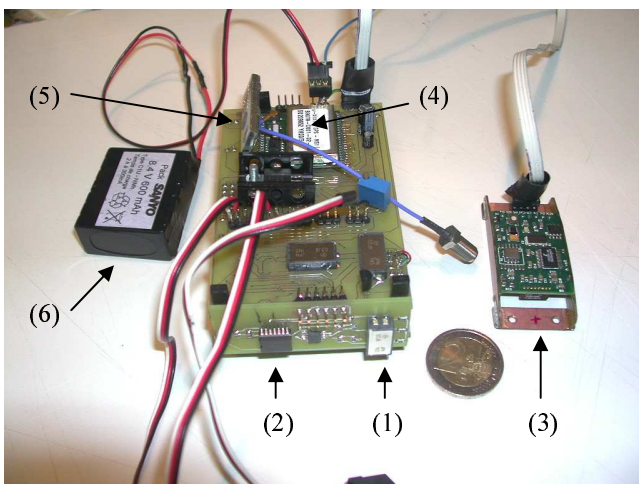


Figure 7 The embedded system

The processing power of our platform is provided by a micro-controller Motorola 68332 which has been mounted on a pseudo-BBC board (60*95 mm) including 32 Kb of ROM and RAM and serial interfaces. This controller allows us to connect easily all our sensors and make future expansion of the system possible.

To evaluate the angular velocity of the Pégase-50 we used 3 piezoelectric Murata gyrometers (1) following the 3 axes of the plane (for the roll, pitch and yaw). They are connected to the calculator through a 4 channels 12 bits ADC which gives us a measure ($\pm 300^\circ/s \rightarrow 0-5V$) at 50Hz (linked to the bandwidth of the sensor).

To acquire acceleration of the MAV we have used two Analog Device ADXL210 (2) placed, as for the gyrometers, following the 3 axes of the plane. They are working at 125 Hz. Furthermore, in order to compensate a temperature drift, presenting with this component and with the gyrometers, we have mounted a temperature sensor connected to the ADC's 4th channel.

We also use a Honeywell three axes magnetic field sensor (3) which lets us have an absolute reference for navigation. This sensor uses a asynchronous serial interface (RS232 19200 Bds) available on the calculator board.

To determine the position, altitude and speed of our plane we used a μ -Blox GPS (4). This component transmits those parameters through another serial interface with an 1Hz acquisition frequency.

The human-in-control system is provided by a standard eight-channel R/C radio system and standard R/C servos (PWM control signals). Three channels are used for control of the MAV – aileron, elevator and propulsion. A fourth channel, which is a toggle switch, is used to switch between human and computer control of the aircraft. The embedded circuit is independent of the calculator systems. So that, in the event of a computer failure, the pilot can still assume the control of the MAV.

So as to record and control actuators, we have connected the micro-controller to the R/C system, using a module of the 68332 which manages PWM signals, and keeping the two systems electrically independent.

We transmit all the flight parameters, with a 9600Bds digital HF transmitter Radiometrix (5), to a ground station which allows us to record and analyze the MAV compartment.

Finally we validated our complete system, which only weights 190g with a 8.4V/500mA NiMh battery (6), in the laboratory. The system is ready for flight test and algorithms implementation.

VIII. CONCLUSION

In this paper a nonlinear model of Pégase-50 is established. The guidance and control laws are presented based on a linearization model. The attitude control law is verified by nonlinear simulation. The further works include:

- to analyse the robustness of the control law
- to identify the fault flight condition model on line and to design reconfigurable control law
- to study the feasibility of open loop control
- to validate algorithms with our embedded system during flight tests

REFERENCES

- [1] Damien BRENOT, Sébastien GORCE, Arnaud Grelou and Laurent PLATEAUX, *Realisation du Micro-Drone Pégase*. Projet d'Initiative Personnelle, 2000
- [2] Guy TOULOUSE, *Activite Microdrone a l'ENSICA 1999-2001*. Département de Mécanique des Fluides.

- [3] M.S. Grewal and A.P. Andrews. *Kalman Filtering – Theory and Practice*. Prentice-Hall, Inc, 1993
- [4] D. H. Titterton and J. L. Weston. *Strapdown inertial navigation technology*. Peter Peregrinus Ltd. , 1997
- [5] Pierre Rebuffet. *Aérodynamique Expérimentale*. Librairie Polytechnique Ch. Béranger, 1962
- [6] E. L. Houghton and N. B. Carruthers. *Aerodynamics for Engineering Students*. Edward Arnold Pty Ltd, 1986
- [7] Salah Sukkarieh. *Low Cost, High Integrity, Aided Inertial Navigation Systems for Autonomous Land Vehicles*. PhD dissertation. The University of Sydney, Mar. 2000

APPENDIX

The twelve degrees nonlinear equation of Pégase is:

$$\left\{ \begin{array}{l}
 \dot{V}_x = \frac{P - F_x \cos \alpha \cos \beta - F_z \sin \alpha - F_y \cos \alpha \sin \beta}{m} - g \sin \theta - V_y r - V_z q \\
 \dot{V}_y = \frac{-F_x \sin \beta + F_y \cos \beta}{m} + g \cos \theta \sin \varphi + V_z p - V_x r \\
 \dot{V}_z = \frac{-F_x \sin \alpha \cos \beta + F_z \cos \alpha - F_y \sin \alpha \sin \beta}{m} + g \cos \theta \cos \varphi + V_x q - V_y p \\
 \dot{p} = \frac{M_x + \Delta w_x + (I_y - I_z + \frac{I_{xz}^2}{I_z})qr - (I_{xz} + \frac{I_{xz}}{I_x(I_x - I_y)})pq + \frac{I_{xz}}{I_z} M_z}{I_x - I_{xz}^2 / I_z} \\
 \dot{q} = (M_y + \Delta w_y + (I_z - I_x)pr - I_{xz}(r^2 - p^2)) / I_y \\
 \dot{r} = (-M_z + \Delta w_z - (I_x - I_y)pq + I_{xz}(-qr + \dot{p})) / I_z \\
 \dot{\psi} = (-r \cos \varphi - q \sin \varphi) / \cos \theta \\
 \dot{\theta} = -r \sin \varphi + p \cos \varphi \\
 \dot{\varphi} = p + \tan \theta (+r \cos \varphi + p \sin \varphi) \\
 \dot{h} = V_x \sin \theta - V_z \cos \theta \cos \varphi - V_y \cos \theta \sin \varphi \\
 \dot{x} = V_x \cos \psi \cos \theta - V_z (\sin \psi \sin \varphi - \cos \psi \sin \theta \cos \varphi) + V_y (\sin \psi \cos \varphi + \cos \psi \sin \theta \sin \varphi) \\
 \dot{y} = -V_x \sin \psi \cos \theta - V_z (\cos \psi \sin \varphi + \sin \psi \sin \theta \cos \varphi) + V_y (\cos \psi \cos \varphi - \sin \psi \sin \theta \sin \varphi)
 \end{array} \right.$$